Available online at www.CivileJournal.org

Civil Engineering Journal

(E-ISSN: 2476-3055; ISSN: 2676-6957)

Vol. 11, No. 01, January, 2025

Comprehensive Assessment for Liquefaction Vulnerability in Indonesia: Empirical and Element Simulation Approaches

Siti Nurlita Fitri [1, 2*], Kazuhide Sawada [1]

[1] Graduate School of Engineering, Gifu University, 1-1 Yanagido, Gifu 501-1193, Japan.

[2] UNSGeoscience Research Group, Civil Engineering Department, Sebelas Maret University, Surakarta 57126, Indonesia.

Received 03 October 2024; Revised 02 December 2024; Accepted 09 December 2024; Published 01 January 2025

Abstract

Historical liquefaction events have occurred at many locations, such as Yogyakarta and Lombok; the most significant flow side is in Palu. The standard Indonesian liquefaction assessment is based on a simplified empirical analysis. However, these methods only occasionally yield appropriate results. Contrastingly, the limited data from the cyclic test ensured that the liquefaction ratio could only partially support the liquefaction vulnerability. This research aims to re-examine the empirical approach that combines the constitutive model using LIQCA with a cyclic triaxial test (CXT) and cyclic simple shear (CSS). The empirical method was arranged using deterministic and probabilistic approaches, and the recommendation of the peak ground acceleration (PGA) threshold was validated. The results show a strong relationship between all calculation methods and the SPT value, which differs in the liquefaction strength ratio. This output offers the PGA recommendation results, reaching a 48% overestimation from the empirical method without considering the cyclic test. This research presents the development of a combination of the empirical method with the element simulation from CXT and CSS. This offers a comprehensive overview of the Indonesian requirement standard assessment for liquefaction vulnerability analysis.

Keywords: LIQCA; Liquefaction; Element Simulation; Empirical; Peak Ground Acceleration; Probabilistic.

1. Introduction

Earthquakes are natural phenomena that have led to disasters and caused destruction in Indonesia. As a seismic-prone country located on several large tectonic plates, namely Indo-Australian, Pacific, and Eurasian plates, a vast number of local faults and thrusts also influence the likelihood of earthquakes. Consequently, many researchers in Indonesia have conducted studies to mitigate the drawbacks of earthquakes in specific areas, focusing on mainshocks and aftershocks [1, 2], as well as ground performance [3] and loss assessments [4]. According to Indonesia Geological Information, the most prominent earthquakes in the past 20 years occurred in Cianjur (2022), Mamuju (2021), Palu (2018), Lombok (2018), Padang (2009), and Yogyakarta (2006). In addition, geotechnical failure, usually induced by earthquakes and causing many deaths and destruction in Indonesia, leads to liquefaction phenomena such as landslides, lateral spreading by liquefaction, and substructure collapse. The most significant of the ground failure phenomena, which included flow slides, lateral spread, settlement, debris floods, and ground slides, was liquefaction from the Palu 2018 earthquake [5, 6].

Liquefaction in Indonesia causes significant destruction for many seismic events. Based on the Geological Department of Indonesia [7], 22 occurrences of liquefaction have been recorded in Indonesia in the last 20 years. For

* Corresponding author: siti.nurlita.fitri.d4@s.gifu-u.ac.jp

http://dx.doi.org/10.28991/CEJ-2025-011-01-019

the Palu 2018 earthquake, there are 375 sites (including Jonooge and Petobo) where seismic intensities are reported, with a maximum value of X on the Modified Mercalli Intensity (MMI) scale [8]. Furthermore, in the Lombok 2018 earthquake, the MMI scale reached VIII values, and the Yogyakarta 2016 earthquake was at the same level. The extent of damage caused by liquefaction events is shown in Figure 1.

(a) (b) (c) (d)

Figure 1. Liquefaction in Indonesia (a) Petobo [9], (b) Jonooge [10], (c) Yogyakarta [11], (d) Lombok [12]

Liquefaction assessments have been comprehensively developed worldwide. General analyses include stress-based, cyclic strain-based, energy-based, laboratory and physical model testing, regional liquefaction hazard maps and historical liquefaction occurrences, field measurements, and computational mechanics approaches [13]. According to Fitri & Sawada [14], liquefaction studies in Indonesia offer the liquefaction potential in stress based on deterministic and probabilistic approaches with a massive number of empirical and semi-empirical analyses. The remaining were soil-site testing and mapping. Furthermore, the Geotechnical Standard in Indonesia (SNI) (2017) [15] states that liquefaction assessment requirements are based on Seed & Idriss (1971) [16]. The technical community has enjoyed the benefits of empirical methods for evaluating liquefaction triggering. However, each method has flaws. The practical community can be enhanced by employing various methods, evaluating the source of any discrepancies in the results, and employing professional judgment to resolve them [13].

A few laboratories cyclic studies that analyzed liquefaction vulnerability in Indonesia have induced a wide range of empirical assessment calculations. In contrast, deterministic empirical approaches occasionally demonstrate inconsistencies in predicting the liquefaction potential when compared with actual data from sites where liquefaction has occurred. Therefore, cyclic laboratory investigations should be conducted. This testing continues to play a critical role in examining and assessing the potential for liquefaction triggering and the influence of acceptable content, density, fines content, grain size distribution, degree of saturation, and nonuniform load cycles. It is also beneficial for establishing constitutive relationships for developing pore pressure prior to liquefaction and to investigate the post-liquefaction behavior of soils. To determine the complexity of the soil behavior in the soil constitutive approach, all models must consider both elastic and inelastic deformations of the soil matrix. This theoretical approach supports the soil material response in examining predictions and modeling in both the field and laboratory [16, 17].

Owing to the limitations of the cyclic equipment test in Indonesia, the constitutive soil model for the element simulating the cyclic test is an alternative for analyzing the dynamic behavior of soil. One of the element simulations using constitutive soil models is the prediction approach of LIQCA. This model used the elastoplastic (E-P) constitutive model Oka et al. [18] and was derived from the following assumptions: degradation of the plastic strain-dependent shear modulus, overconsolidation of the boundary surface, infinitesimal-strain theory, elastoplastic theory, generalized non-associated flow rule, nonlinear kinematic hardening rule, and fading memory of the initial anisotropy [19]. This method has been used in a wide range of Japanese soil analyses for liquefaction, such as desaturated silica sand for cyclic tests, applying probabilistic models to structural and material strength, and investigating the primary cause of the subsidence of road embankments at survey sites using a numerical model [20-22].

Diverse thresholds for the permitted peak ground acceleration (PGA) have been identified in numerous seismic zonation guidelines and building regulations [23]. The differences in the recommendation values based on historical events also boost the PGA threshold. For a simplified approach, the PGA plays a significant role in assessing the liquefaction shear that produces the FS value in the deterministic method. Furthermore, the results of the probabilistic approach were shown in the ground description through an analysis of the FS. This study aims to analyze a simplified stress-based approach to liquefaction-triggering assessment, that combines the constitutive model using LIQCA with the comprehensive simulation of the cyclic triaxial test (CXT) and cyclic simple shear (CSS). The performance of the cyclic simulation test with PGA variants produced the recommended value to ensure the safety condition, which can be validated by the probabilistic method to offer the response description. The proof of the percentage simulation of CXT and CSS with the empirical method is expected to fill the gap in Indonesian requirement assessment for liquefaction vulnerability analysis.

1.1. Overview of Earlier Studies

Assessments of liquefaction vulnerability in Indonesia can be classified into several approaches. Field measurements and regional examinations were conducted by Jalil et al. [24] using microtremor measurements, in which the shear wave velocity and ground shear strain approaches were combined with the site characteristics to assess liquefaction. Moreover, Swedish weight sounding (SWS) and standard penetration text (SPT) were analyzed to obtain the liquefaction index. Another method is site reconnaissance, which uses Google StreetView and historical evidence to observe ground failures caused by liquefaction [5]. However, the recalculation focused only on site-specific liquefaction evidence and used an empirical estimation. The complex soil behavior at different sites must be captured.

The general analysis has been dominated by SPT and CPT for empirical and semi-empirical analyses to conduct liquefaction indexing. Mase [11] proposed a simplified energy concept with one-dimensional earthquake response research to identify the maximum ground acceleration combined with potential indexing for liquefaction. Aini et al. [25] focused on calculating the liquefaction potential index (LPI), and Zakariya et al. [26] examined several indexing liquefactions using five different indexing approaches. The results showed that the LPI and liquefaction reduction number (LRN) were more developed for the probability of the appearance of liquefaction. In contrast, the liquefaction risk index (LRI) and liquefaction severity index (LSI) focus on the degree of risk and level of liquefaction destruction. Empirical and semi-empirical methods dominate all project liquefaction vulnerability studies in Indonesia because the Indonesian standard [15] requires a simplified approach following Idriss & Boulanger (2008) [27] and Youd & Idriss (2001) [28]. However, the empirical methods are based on historical data and may not be applicable to all soil types or loading conditions. There are limitations to verifying the accuracy of these empirical models and refining them based on the observed real soil site behavior.

Liquefaction occurs because of earthquakes; hence, ground motion analysis is an essential approach for its examination. The common method is a deterministic and probabilistic seismic hazard analysis (DSHA and PSHA, respectively) that propagates time-historical waves to the ground surface [29, 30]. The output is a combination of the maximum acceleration (PGA) for the seismic wave analysis, earthquake magnitude, N-SPT value from the boring test, and various soil properties, which are evaluated using a semi-empirical technique to determine the liquefaction safety factor. Nonetheless, this research does not fully address the specific range of PGA values and their influence on the empirical analysis.

The limited number of laboratory experiments regarding soil cyclic tests and dynamic load models in Indonesian liquefaction research has led to few references. Kiyota et al. [31] conducted undrained triaxial cyclic measurements on in situ undisturbed samples of Indonesian soil and determined the cyclic resistance ratio of the reported liquefied soil. Moreover, Mase [32] analyzed a shaking table experiment and found that the dynamic load variation significantly affected the time stages of liquefaction, the increase in the percentage of liquefaction duration, and the cyclic stress ratio. However, there is a limited amount of cyclic equipment for dynamic analysis in Indonesia, and it is difficult to prevent undisturbed samples from being used for actual site conditions. Soil cyclic simulations require complementing and enhancing other methods to provide a more comprehensive understanding of critical liquefaction events.

CXT and CSS are alternative laboratory experiments for determining the liquefaction behavior of soil samples. Khashila et al. [33] found that CXT simulates conditions that are more representative of isotropic stress states, whereas CSS better mimics the shear stresses experienced during seismic events. Arriaga & Green [34] showed that the CXT evaluates soil behavior under three-dimensional stress conditions, whereas CSS focuses on two-dimensional shear stress. The cyclic strain approach effectively evaluated the triggering of liquefaction. Önalp et al. [35] described CXT and CSS as useful for assessing soil liquefaction; CSS is particularly convenient and rapid for confirming judgments, although physical properties must also be considered. An evaluation of the liquefaction strength of Japanese natural sandy soil using triaxial and simple shear tests was also completed by Oka et al. [36]. Nevertheless, significant differences from the existing liquefaction criteria were observed. This lack of comprehensive data may hinder our ability to draw definitive conclusions regarding the liquefaction potential under various soil conditions. CXT and CSS results require proper correlation and validation for field simulations.

Soil element simulations based on constitutive models are valuable tools for predicting soil liquefaction because the essential outputs provide complex soil behaviors, offer different soil states, and simulate dynamic loading and effective stress. Sternik [37] developed an elastic-plastic model incorporating the Drucker-Prager failure criterion, a nonassociated plastic flow rule, and deviatoric hardening that is suitable for simulating soil elements in liquefaction tests. In addition, some previous studies presented a constitutive model with a shear-history threshold that accurately predicted the cyclic strength of sand under various cyclic stress ratios by incorporating a shift in the apparent angle of phase transformation and a deviatoric fabric tensor [27, 28]. Fujiwara et al. [38] used LIQCA to generate a simulated stress-strain relationship and an effective stress path for liquefiable sand. Moreover, Oka et al. [36] described many constitutive models for sand and liquefiable soil, such as cyclic EP and elasto-viscoplastic models, and provided further approaches for estimating liquefaction based on dynamic analysis. However, future research should focus on refining these models to capture the behavior of soils under various loading scenarios more accurately. In addition, there is a need for an extensive field validation of the LIQCA method using data from recent earthquakes. This condition involves calibrating the model against the observed liquefaction events to enhance its predictive capabilities.

Based on all further research suggestions and limitations from the previous literature, this research provides the development of a combination of the empirical method typically used in Indonesia with element simulation from the CXT and CSS, which results in several historical examples of liquefaction in Indonesia. Furthermore, the results from the simplified methods of Idriss & Boulanger (2008) [27] and Youd & Idriss (2001) [28] and soil sample simulations were validated by the involvement of the PGA value to determine the range of the threshold of the two approaches. This output expands the Indonesia Geotechnical Standard for liquefaction assessment to include an appropriate approach for conducting cyclic soil tests.

2. Research Methodology

2.1. Research Location

This study used specific locations in Indonesia with historical liquefaction phenomena, namely Lombok, Yogyakarta, and Palu areas. The primary investigation is from the Indonesia liquefaction map, which considers the seismic and geological characteristics of a particular site. In addition, the seismic factor uses the 10% probability of an earthquake in 50 years for liquefaction analysis, where the lithology factor considers non-cohesive sites and loose and saturated conditions. The geomorphology and hydrogeology were also examined. The detailed locations and overlays of the liquefaction vulnerability map are shown in Figure 2.

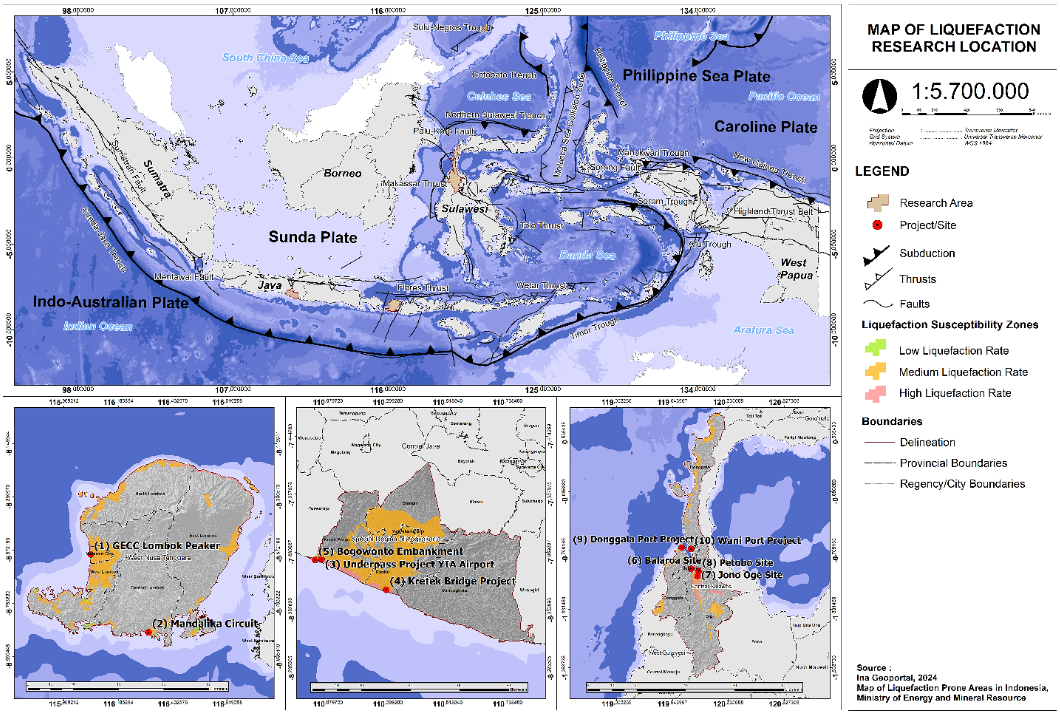

Figure 2. Soil sample location

Figure 2 shows the soil sample locations used in this research. This study utilized specific locations in Indonesia with high and medium liquefaction susceptibilities. According to the Geology Department of Indonesia [7], the liquefaction zone is highly susceptible to destruction, such as flow slides, lateral spreading, settlement and tilting, and sand boiling. A medium liquefaction rate indicates lateral spreading, settlement, tilting, and sand boiling. The locations are on one of three islands: Java Island in the Special Region of Yogyakarta Province, Lombok Island in East Nusa Tenggara Province, and Sulawesi Island in Central Sulawesi Province. The details of the locations, number of boreholes, and element simulations are presented in Table 1.

Table 1. Soil sample location

No of project/ site	Location	Province	No. boreholes	Name of BH	No of soil sample	Location	Area
1	GECC Lombok Peaker	East nusa tenggara/ Lombok Island	4	BH1, BH2, BH3, BH4	20	1	Lombok
2	Mandalika circuit	East nusa tenggara/ Lombok Island	5	BH5, BH6, BH7, BH8, BH9	21	2	Lombok
3	Underpass project YIA airport t	Special region of Yogyakarta	4	BH10, BH11, BH12, BH13	20	3	Yogyakarta
4	Kretek bridge project	Special region of Yogyakarta	9	BH14, BH15, BH16, BH17, BH18, BH19, BH20, BH21, BH22	47	4	Yogyakarta
5	Bogowonto embankment	Special region of Yogyakarta	3	BH23, BH24, BH25	15	5	Yogyakarta
6	Balora site	Central Sulawesi/Palu	5	BH26, BH27, BH 28, BH29, BH30	20	6	Palu
7	Jonooge site	Central Sulawesi/Palu	10	BH31, BH32, BH33, BH34, BH35, BH36, BH37, BH38, BH39, BH40	41	7	Palu
8	Petobo site	Central Sulawesi/Palu	4	BH41, BH42, BH43, BH44	19	8	Palu
9	Donggala port project	Central Sulawesi/Palu	3	BH45, BH46, BH47	7	9	Palu
10	Wani Port project	Central Sulawesi/Palu	3	BH48, BH49, BH50	10	10	Palu
Total			**50**		**220**		

Table 1 shows the soil sample locations divided into the three provinces and areas. All boring points were from the SPT (Standard Penetration Test) site investigation with the limitation of soil sample with the saturated condition, loose sand classification, and NSPT <20 because it indicates the possibility of liquefaction [39]. The first area is Lombok Island with two points, the GECC Lombok Peaker and Mandalika circuit, with four and five boreholes and a total of 20 and 21 soil samples, respectively. In the Yogyakarta area, the projects are the Underpass YIA airport, Kretek Bridge Project, and Bogowonto embankment, with total borehole points being 4, 9, and 3 with 20, 47, and 15 soil samples, respectively. The rest of the locations in the Palu region have five sites and projects, namely Balora, Jonooge, Petobo, Donggala Port, and Wani Port, with a total of 5, 10, 4, 3, and 3 boreholes, and a total of 20, 41, 19, 7, and 10 soil samples, respectively. The total number of boreholes from three provinces was 50, and the total number of soil samples was 220.

2.2. Research Diagram

The first step in research flow analysis was to examine areas with the possibility identified from the liquefaction susceptibility map of Indonesia. Thus, a historical event of liquefaction occurrence and a field investigation after each phenomenon should have been conducted. The research procedure is illustrated in Figure 3.

2.3. Site Investigation and Soil Sample

As described in the previous section, an SPT investigation was conducted in all research locations. The soil sample was also filtered using sand classification and groundwater table data, as well as the limitation of the density of the layer (NSPT < 20). Furthermore, other properties of the soil parameters should be determined by soil tests or estimates, depending on the test or empirical correlation.

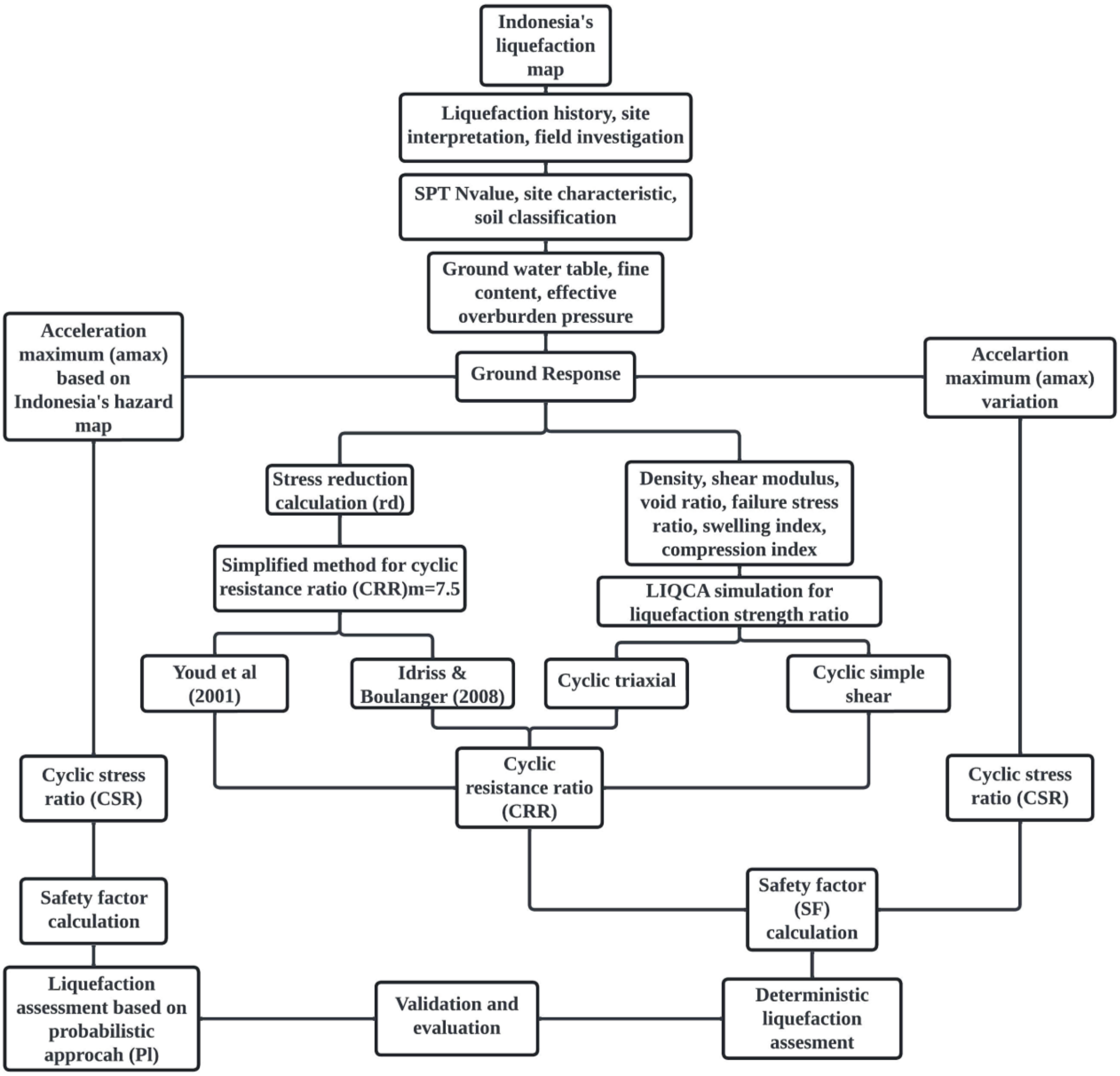

Figure 3. Research flowchart

2.4. Ground Response

The ground response assessment used to calculate liquefaction potential in this research was divided into two criteria. The first approach was to examine the effect of liquefaction strength from an element simulation, which LIQCA provides with the determined value of PGA from the Indonesia Earthquake hazard map [40]. The three areas exhibited different maximum accelerations. Based on this map, this study utilized an earthquake probability of 10% in 50 years. The values ranged from 0.3 to 0.46 g for the Lombok area, 0.46 g for the Yogyakarta area, and 0.6 g for the Palu location, respectively. Moreover, Irdhiani et al. [30] conducted a field investigation of PGA in the Palu area site at the value of 05-0.6 g. The values from the hazard map were adequate. According to Orense [41], liquefaction may occur when the PGA is more significant than 150 gals (0.15 g) and the PGV is greater than 20 kine, as indicated by the analyses of significant motion records at multiple locations. Hence, this range of data supports the idea that all locations have a high liquefaction potential.

2.5. LIQCA Constitutive Model for Element Simulation

The LIQCA constitutive soil parameters are applied to generate a simulation element. The (EP) model is a fundamental numerical analysis tool for this program. In addition, the soil properties required for the input are the void ratio (e_o), Poisson's ratio (v), compression index (k), swelling index (λ), overconsolidation ratio (OCR), shear modulus (G_0), density (D_r), failure stress ratio (M_r), dilatancy parameter (n), and reference strain (γ_{ref}^{E}). The basic experiment entailed obtaining these parameters with empirical soil mechanical correlation if the secondary data were unavailable.

The E-P model was applied to liquefiable soil layers with the potential for liquefaction. In addition, the model was implemented in soil layers, including non-liquefiable layers located near the ground surface and an embankment, that can produce extensive strain. An element simulation attempted to replicate the findings of mechanical laboratory tests, including simple shear and triaxial tests. A particular constitutive model can be incorporated into the computer program to conduct elemental simulation. Furthermore, the concerns for this method are the initial shear modulus ratio and deformation mode. It is essential to consider the strain standard and background before achieving the strain standard. This has a substantial impact on the anticipated deformation. Certain parameters in the E-P model substantially affect the possibility of increases in the shear strain and decreases in effective stress. The simulation for the cyclic experimental tests was conducted based on the material using elastoplastic approaches in a controlled test with the initial effective stress of the site from the soil sample taken under undrained conditions. The detailed calculation was adopted from the LIQCA Research and Development Group [19]; it can be explained as follows:

- ***Cyclic Simple Shear (CSS) Test***

The undrained simple shear simulation has been conducted following the assumption:

$$d\varepsilon_x = d\varepsilon_y = d\varepsilon_z = 0 \tag{1}$$

Based on the relationship between the strain increment vector ($d\varepsilon_i$), elastoplastic matrix (D_{ij}), and stress increment vector ($d\sigma_i$) in three dimensions, which offers shearing in x and y directions, the calculation is analyzed with the initial form:

$$\begin{bmatrix} d\sigma_x \\ d\sigma_y \\ d\sigma_{xy} \\ d\sigma_z \end{bmatrix} + \begin{bmatrix} R_x \\ R_y \\ R_{xy} \\ R_z \end{bmatrix} = \begin{bmatrix} D_{11} & D_{12} & D_{13} & D_{14} \\ D_{21} & D_{22} & D_{23} & D_{24} \\ D_{31} & D_{32} & D_{33} & D_{34} \\ D_{41} & D_{42} & D_{43} & D_{44} \end{bmatrix} \begin{bmatrix} d\varepsilon_x \\ d\varepsilon_y \\ d\varepsilon_{xy} \\ d\varepsilon_z \end{bmatrix} \tag{2}$$

where R is the modified stress vector at failure. Owing to the assumptions of the CSS test, the applied equation was changed as follows:

$$\begin{bmatrix} d\sigma_x \\ d\sigma_y \\ d\sigma_{xy} \\ d\sigma_z \end{bmatrix} + \begin{bmatrix} R_x \\ R_y \\ R_{xy} \\ R_z \end{bmatrix} = \begin{bmatrix} D_{13} & d\varepsilon_{xy} \\ D_{23} & d\varepsilon_{xy} \\ D_{33} & d\varepsilon_{xy} \\ D_{43} & d\varepsilon_{xy} \end{bmatrix} \tag{3}$$

According to the stress control test, the deformation can be calculated using the matrix in Equation 3, whereas another stress increment can be analyzed using the following formula:

$$d\varepsilon_x = \frac{d\sigma_{xy} + R_{xy}}{D_{33}} \tag{4}$$

In undrained conditions, the relationship between stress and strain increments is:

$$d\sigma_x = d\sigma_y = d\sigma_z = 0 \tag{5}$$

To solve the formula, the load input in the stress control test used stress increment $d\sigma_{xy}$ as a load in the modified matrix.

$$\begin{bmatrix} 0 \\ 0 \\ d\sigma_{xy} \\ 0 \end{bmatrix} + \begin{bmatrix} R_x \\ R_y \\ R_{xy} \\ R_z \end{bmatrix} = \begin{bmatrix} D_{11} & D_{12} & D_{13} & D_{14} \\ D_{21} & D_{22} & D_{23} & D_{24} \\ D_{31} & D_{32} & D_{33} & D_{34} \\ D_{41} & D_{42} & D_{43} & D_{44} \end{bmatrix} \begin{bmatrix} d\varepsilon_x \\ d\varepsilon_y \\ d\varepsilon_{xy} \\ d\varepsilon_z \end{bmatrix} \tag{6}$$

- ***Cyclic Triaxial (CXT)Test***

The general matrix for a cyclic test using the elastoplastic approach is presented in Equation 2. The unconsolidated undrained triaxial simulation matrix was based on several assumptions.

$$d\varepsilon_{xy} = d\varepsilon_{xy} = 0 \tag{7}$$

$$d\sigma_x = d\sigma_z = 0 \tag{8}$$

$$d\varepsilon_x = d\varepsilon_z = -\frac{1}{2} d\varepsilon_y \tag{9}$$

Therefore, the general matrix in Equation 2 can be improved as follows.

$$\begin{bmatrix} d\sigma_x \\ d\sigma_y \\ 0 \\ d\sigma_z \end{bmatrix} + \begin{bmatrix} R_x \\ R_y \\ R_{xy} \\ R_z \end{bmatrix} = \begin{bmatrix} D_{11} & D_{12} & D_{13} & D_{14} \\ D_{21} & D_{22} & D_{23} & D_{24} \\ D_{31} & D_{32} & D_{33} & D_{34} \\ D_{41} & D_{42} & D_{43} & D_{44} \end{bmatrix} \begin{bmatrix} -\frac{1}{2} d\varepsilon_y \\ d\varepsilon_y \\ 0 \\ -\frac{1}{2} d\varepsilon_y \end{bmatrix} \tag{10}$$

For the stress control test, the deviator increment stress is given by Equation 11:

$$dq = d\sigma_y - d\sigma_z \tag{11}$$

Equation 10 is modified by Equation 11 in the first and second lines, and the relationship increment between the stress and strain is obtained. Moreover, another equation for the stress increment after the strain can be calculated as follows:

$$d\varepsilon_y = \frac{dq+(R_y - R_x)}{(-\frac{1}{2}D_{21}+D_{22}-\frac{1}{2}D_{24}+\frac{1}{2}D_{11}-D_{12}+\frac{1}{2}D_{14})} \tag{12}$$

Owing to the undrained condition, the assumption is given in Equation 13, and the general equation is changed to Equation 14:

$$d\sigma_{xy} = d\varepsilon_{xy} = 0 \text{ and } d\sigma_x = d\sigma_z = 0 \tag{13}$$

$$\begin{bmatrix} 0 \\ d\sigma_y \\ 0 \\ 0 \end{bmatrix} + \begin{bmatrix} R_x \\ R_y \\ R_{xy} \\ R_z \end{bmatrix} = \begin{bmatrix} D_{11} & D_{12} & D_{13} & D_{14} \\ D_{21} & D_{22} & D_{23} & D_{24} \\ D_{31} & D_{32} & D_{33} & D_{34} \\ D_{41} & D_{42} & D_{43} & D_{44} \end{bmatrix} \begin{bmatrix} d\varepsilon_x \\ d\varepsilon_y \\ 0 \\ d\varepsilon_z \end{bmatrix} \tag{14}$$

2.6. Simplified Stress-Based Approach

The simplified method in this study collected data from boreholes at several locations, and the SPT interpretation was the first screening to determine the soil layer. The corrected SPT blow count apparent sand equivalence was $(N_1)_{60cs}$. The correction factor was based on that used by Youd & Idriss (2001) [28]. All the empirical analysis were calculated from the SPT, and the next step was to calculate the factor for stress reduction (rd) depending on the depth (z).

$$rd = \frac{1-0.4113z^{0.5}+0.04052z+0.001753z^{1.5}}{1-0.4177z^{0.5}+0.05729z^{1.5}+0.00121z^2} \tag{15}$$

After obtaining the stress reduction factor (rd) from each layer, the effective vertical pressure (σ_{v0}') and total vertical stress (σ_{v0}) were calculated. Thus, the cyclic stress ratio (CSR) was obtained by combining PGA with acceleration max (a_{max}) and gravity (g).

$$CSR_{M;\sigma'v} = 0.65\frac{a_{max}}{g}\frac{\sigma_{v0}}{\sigma_{v0}'}rd \tag{16}$$

The calculation of cyclic resistance ratio (CRR) is depend on the $(N_1)_{60cs}$ of the SPT based on Idriss & Boulanger [27], as follow:

$$CRR_{M=7.5}; = \exp\left(\frac{(N_1)_{60cs}}{14.1} + \left(\frac{(N_1)_{60cs}}{126}\right)^2 - \left(\frac{(N_1)_{60cs}}{23.6}\right)^3 + \left(\frac{(N_1)_{60cs}}{25.4}\right)^2 - 2.8\right) \tag{17}$$

The $CRR_{M=7.5}$ means that the procedure for liquefaction from the empirical approach for an earthquake magnitude of 7.5. The magnitude of the earthquake was calculated using the magnitude scaling factor for correction. In addition, this question also considers the effective stress overburden under the 1 atm condition. Another CRR calculation in this study was estimated using an equation related to Youd & Idriss (2001) [28]:

$$CRR_{M=7.5} = \frac{1}{34-(N_1)_{60cs}} + \frac{(N1)_{60cs}}{135} + \frac{50}{[10(N_1)_{60cs}+45]^2} \tag{18}$$

The final value examine the safety factor (FS) from the CRR and CSR:

$$FS = \frac{CRR_{M=7.5}}{CSR} \tag{19}$$

2.7. Liquefaction Analysis Based on Probabilistic Approach

The probability assessment of liquefaction is conducted using the equation based on Juang et al. [44] which is presented as follow:

$$PL = \frac{1}{1+exp(7.545\,(FS-0.952))} \tag{20}$$

After calculating the empirical method to examine the probability of liquefaction, the value of PL is based on the described conditions. The range of the PL definitions area is presented in Table 2.

Table 2. Liquefaction classifications assigned according to the possibility of liquefaction [45]

Grade	Liquefaction probability	Description
1	PL≤ 0.15	Nearly certain that its non-liquefaction
2	0.15< PL≤0.35	Unlikely to experience liquefaction
3	0.35<PL≤0.65	There is an equal chance of liquefaction and non-liquefaction.
4	0.65<PL≤0.85	Most likely that it will eventually liquefy
5	PL>0.85	Nearly certain to liquefy

3. Results and Discussion

Following the research flowchart in Figure 3, the outputs for each stage of the study areas follow.

3.1. Numerical Analysis for CXT and CSS

The 220 soil samples were simulated using the LIQCA constitutive model for the element simulation of the CXT and CSS. One of the Kretek Bridge Project Yogyakarta simulation results for BH12 is shown in Figure 4 for the CSS and Figure 5 for the CXT. In the CXT, the criterion for liquefaction was the occurrence of a double-amplitude shear strain of 5% (DA5%) and a double-amplitude strain of 7.5% (ɣDA = 7:5%) in the CSS and confining pressure was applied for σ'_c = 2/3 x overburden pressure in-situ for all tests [46, 47].

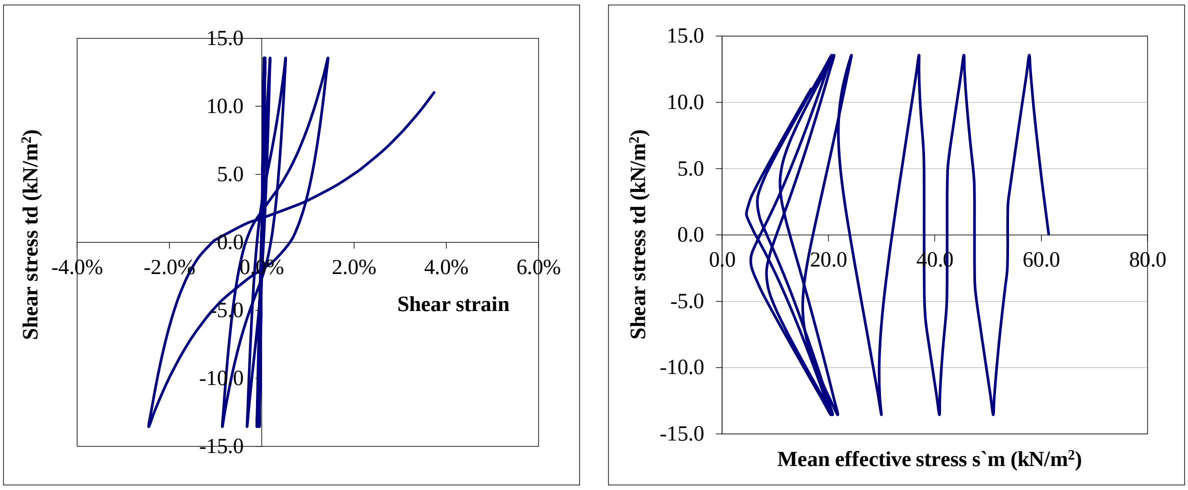

Figure 4. Cyclic simple shear result (CSS) element simulation

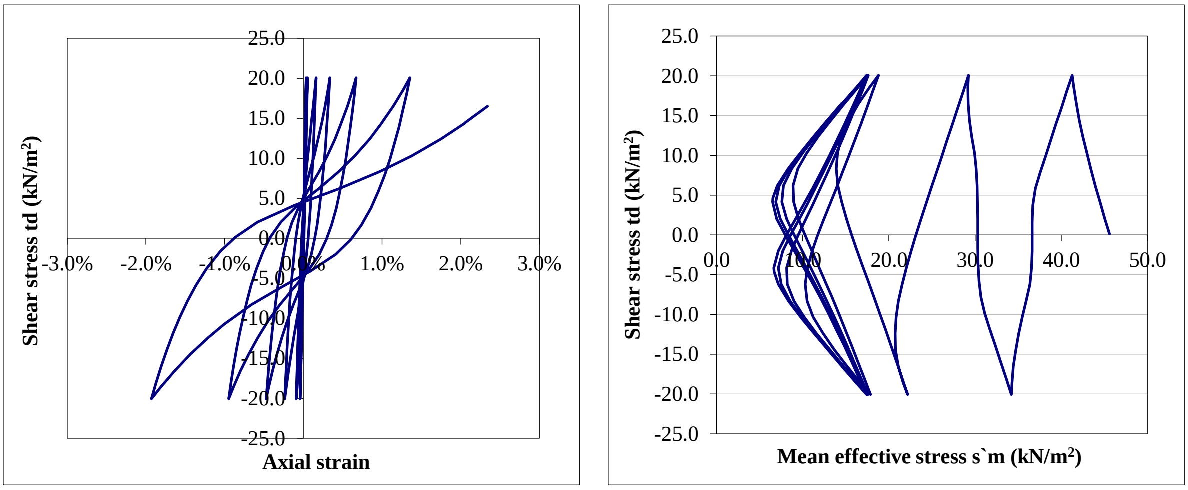

Figure 5. Cyclic triaxial result (CXT) element simulation

As shown in Figures 4 and 5, the output from the CXT and CSS requires a different approach because of the primary load parameters and matrix simulations with the stress ratio test. The stress ratio was used because Arriaga & Green [34] noted that the strain-based approach produces less precise predictions than stress-based methods. Although the two cyclic tests produced the CRR, the CSS simulations presented the shear strain output, whereas CXT was an axial strain in correlation with the applied shear stress. This is because CXT creates an approach that represents the three-dimensional stress state, whereas CSS uses horizontal shear stress with vertical stress under constant conditions. The two methods have limitations in representing field sample situations; specific soil types and engineering interventions are necessary to better understand cyclic soil behavior.

The output of the liquefaction strength ratio based on the simulation of the CSS ranged between 0.09 to 0.28 in the Lombok and Yogyakarta areas, whereas Palu was 0.07 to 0.28. Furthermore, for CXT result simulation for Lombok, Yogyakarta, and Palu areas, the output ranged between 0.26–0.48, 0.23–0.48, and 0.26–0.48, respectively. It is suitable for Nong et al. [48], who was discovered that the liquefaction resistance in CXT was consistently greater than that in CSS. Moreover, the result of liquefaction strength from the Palu site is consistent with Artati et al. [49], who reported the value is approximately 0.26 with various densities. For the Yogyakarta area, the research shows a suitable output, which agrees with Mase et al. [42], with the Prambanan temple in the Yogyakarta area having a range liquefaction ratio of 0.34–0.46.

The relationship between CXT and CSS in all areas is shown in Figure 6. There was a strong correlation between CXT and CSS, with the Pearson correlation coefficient reaching 0.7168. Thus, the connection between the two-sample data was satisfactory. However, the value of liquefaction is not equal for every sample because simple shear and triaxial tests perform shear stress evaluations on various planes. During the CXT, shear stresses were assessed on the plane at a 45° angle from the horizontal and vertical planes. A simple torsional shear test was conducted on a horizontal plane. Although the simulation was based on a constitutive soil model approach, a similar trend was observed for the Japanese soil liquefaction ratio [36].

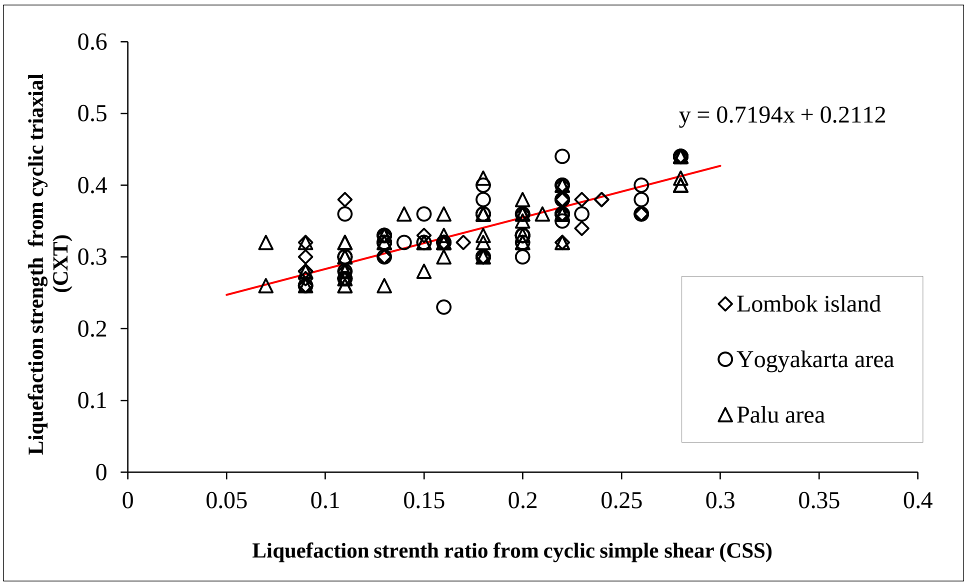

Figure 6. Comparison of liquefaction ratio between cyclic simple shear and cyclic triaxial

3.2. Empirical Method Based on Deterministic Approach and Element Result Simulation

The liquefaction strength ratio was calculated from the empirical method using ay deterministic approach based on Idriss & Boulanger (2008) [27] and Youd & Idriss (2001) [28]. Furthermore, to expand the assessment, the liquefaction ratio from the constitutive soil approach through a cyclic test simulation was combined with an empirical analysis. All results are depicted in Figure 7.

Based on Figure 7, the correlation between the CRR and SPT Value correction $(N_1)_{60cs}$ tended to be similar for all approaches. Idriss & Boulanger [50] offered the same the correlation. The calculation results for all locations show a strong relationship between the empirical calculations and $(N_1)_{60cs}$. The Pearson correlation was higher than that of the constitutive soil approach (CXT and CSS), although all the result had a value greater than 0.6. This is because the empirical method is predicted directly by the SPT correlation, whereas CXT and CSS require more specific data to predict the behavior of soil elements. The relative density is a determinant of the normalized curves, which increase as the density increases [51]. However, slightly different conditions are shown in Location 7 in Figure 7-g, which has the most data from all projects (40 soil sample simulations). The value of the Pearson correlation is in a narrow range from all categories, namely 0.63–0.79. The minimum value of the empirical correlation (Idris-Boulanger simplified) was also predicted at this location at 0.79. Contrastingly, the minimum data of soil simulation provides a higher Pearson correlation at Locations 9 and 10 in Figures 7-i and 7-j, although the differences in the soil sample are not too large. Thus, at significant number of sample data influenced the performance of both correlations in the empirical and simulation methods. However, the constitutive model performs the relatively stable Pearson correlation with a range of 0.61–0.69, excluding Locations 9 and 10 in Figures 7-i and 7-j during the empirical offers more fluctuating data because all data trendline in this research uses linear regression. However, the initial empirical equation is exponential.

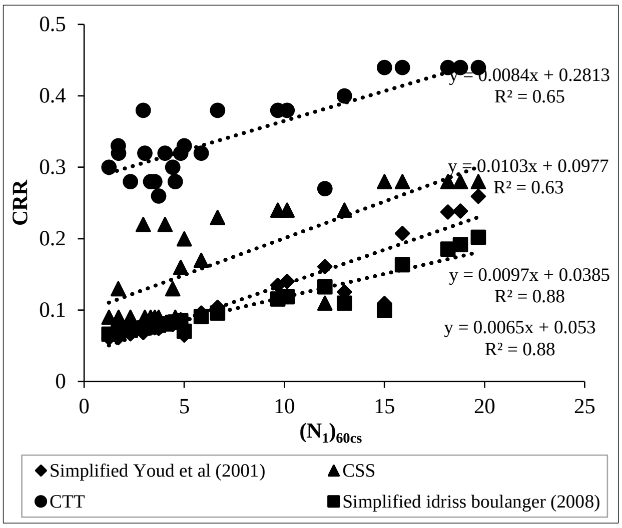

(a)

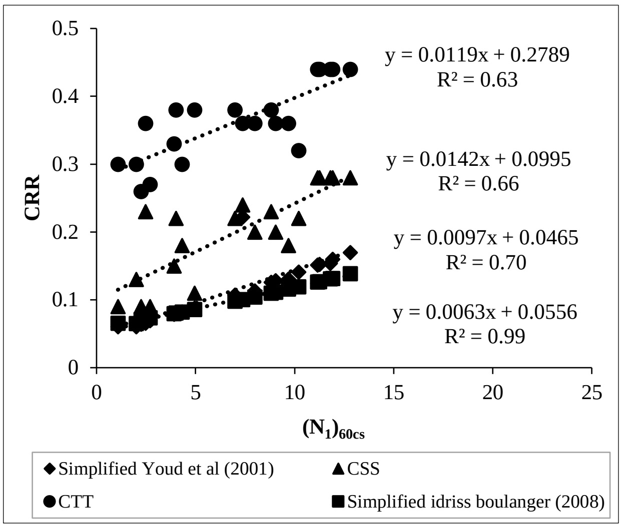

(b)

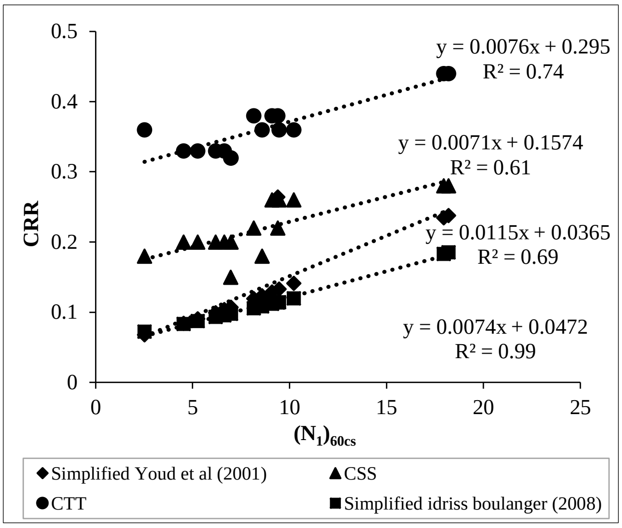

(c)

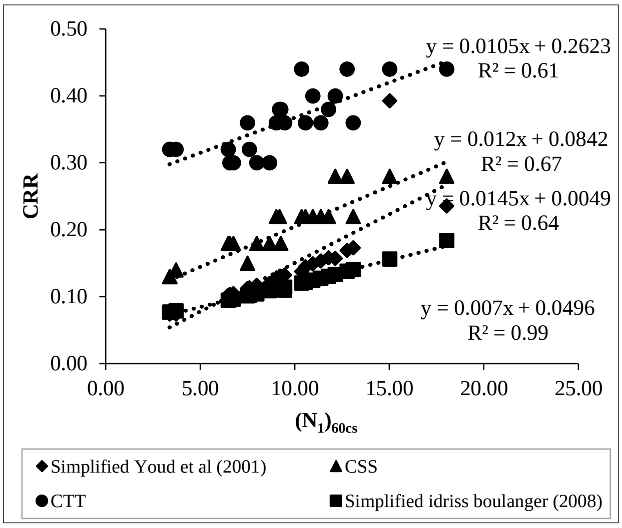

(d)

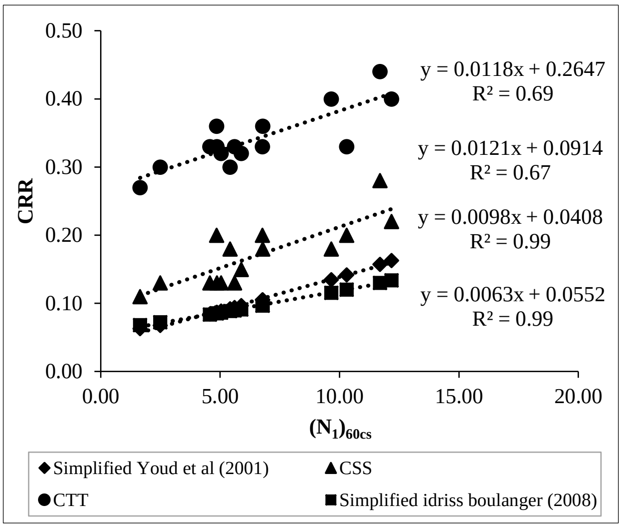

(e)

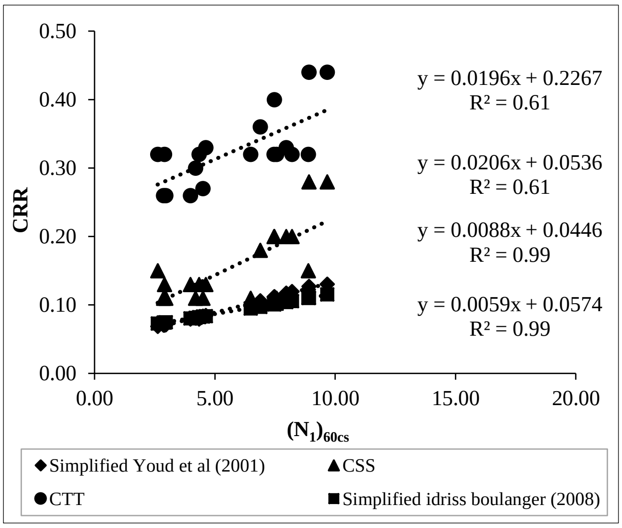

(f)

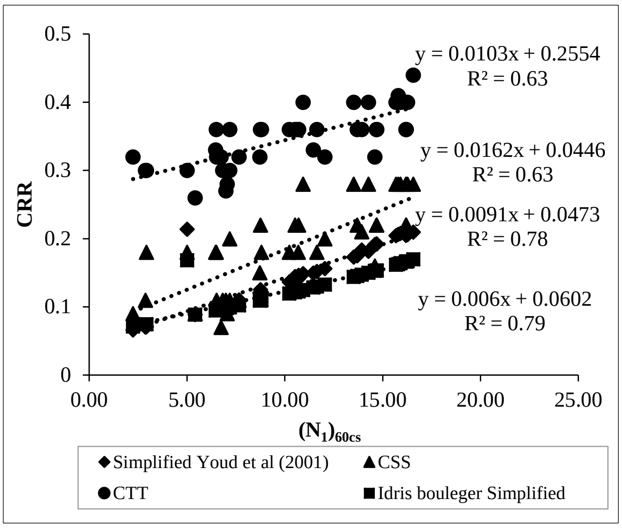

(g)

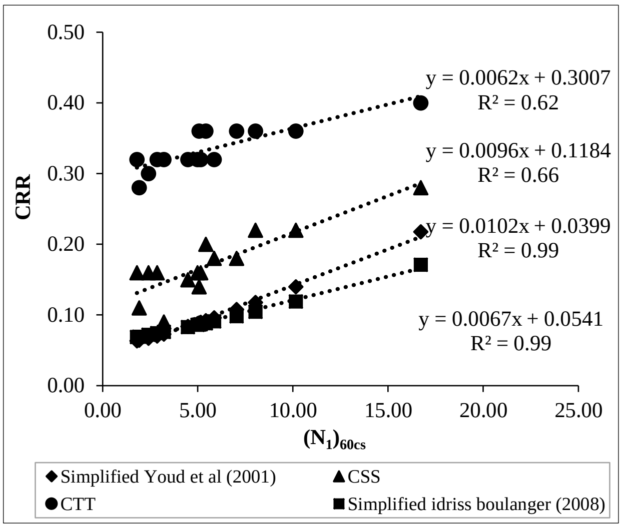

(h)

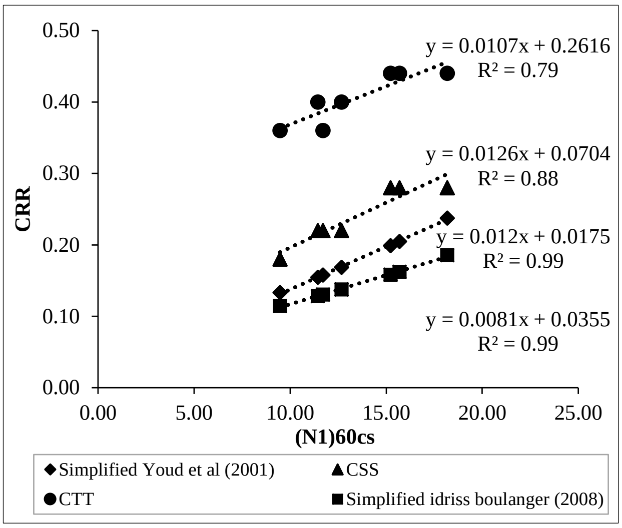

(i)

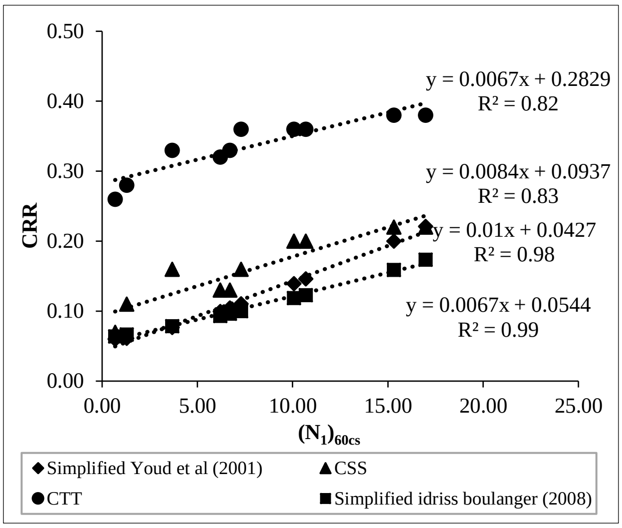

(j)

Figure 7. Liquefaction strength ratio (a) Location 1, (b) Location 2, (c) Location 3, (d) Location 4, (e) Location 5, (f) Location 6, (g) Location 7, (h) Location 8, (i) Location 9, (j) Location 10

The correlation between the corrected SPT value and liquefaction ratio was also shown by Boulanger & Idriss [52] and Chen et al. [53]. Although the SPT data were utilized until the great value reached (N1)60cs = 40, and considering the PL, the specified region in Indonesia is not mentioned. As previously mentioned, this research only focuses on SPT under 20 with actual Indonesian site investigations. Although Location 9 provided the minimum dataset for correlation, it did not generate the maximum substantial value for the Pearson correlation. In contrast, a stronger correlation was found between Location 10 and a higher number of soil samples. Hence, it is not strongly suggested that an increased number of soil properties directly decrease the correlation, although all correlations only generate Pearson correlations of>0.6. This suggests that a considerable number of soil properties and a case history of Indonesia should be gathered to obtain a satisfactory correlation.

The study implements Pearson's correlation to evaluate the methods; however, the correlation tends to decrease as the volume of data increases. Statistical tests become more sensitive to minor effects as sample size increases. This enhanced sensitivity can facilitate the identification of correlations that are less evident in smaller datasets [54]. The 220 data samples in the correlation with $(N_1)_{60\ cs}$ do not offer a strong relationship in linear regression; however, Oka et al. [36] recommended that future research regarding the correlation with other parameters such as preloading history and fines content is suggested to provide better results of soil cyclic behavior.

The slope of the liquefaction ratio in empirical exhibited narrow range between the two approaches for all locations. In fact, the element simulation presented a slope slightly that was slightly more significant than the empirical slope against the SPT value correction $(N_1)_{60cs}$. For the small $(N_1)_{60cs}$ conditions, the CSS provided an almost adequate ratio among two empirical correlations in Location 7. The empirical value indicates a similar value between the two approaches at all locations, excluding Location 9. The larger the $(N_1)_{60cs}$ is, the more significant the gap between the criteria. This analysis used $(N_1)_{60cs}$ under 20 because Hanindya et al. [55] showed the possibility of liquefaction in Palu, although this did not occur because of the rarity of liquefaction at depths exceeding approximately 20 m.

3.3. Peak Ground Acceleration (PGA) Threshold

FS calculations were conducted for various numbers of PGAs; the results are shown in Figure 8. The CXT simulation exhibited the highest CRR. Consequently, all FS values for all PGAs in CXT had the highest output. In this analysis, the minimum FS required is 1.00 because, according to Bhutani & Naval [56], FS values greater than one indicate that soil resistance to liquefaction overcomes the stress imposed by an earthquake, and consequently, soil failure is not anticipated. The increased FS in this approach implies that the soil is more resistant to failure. However, the empirical method slightly overestimated the liquefaction prediction. The FS performance at all locations exhibited the lowest liquefaction prediction.

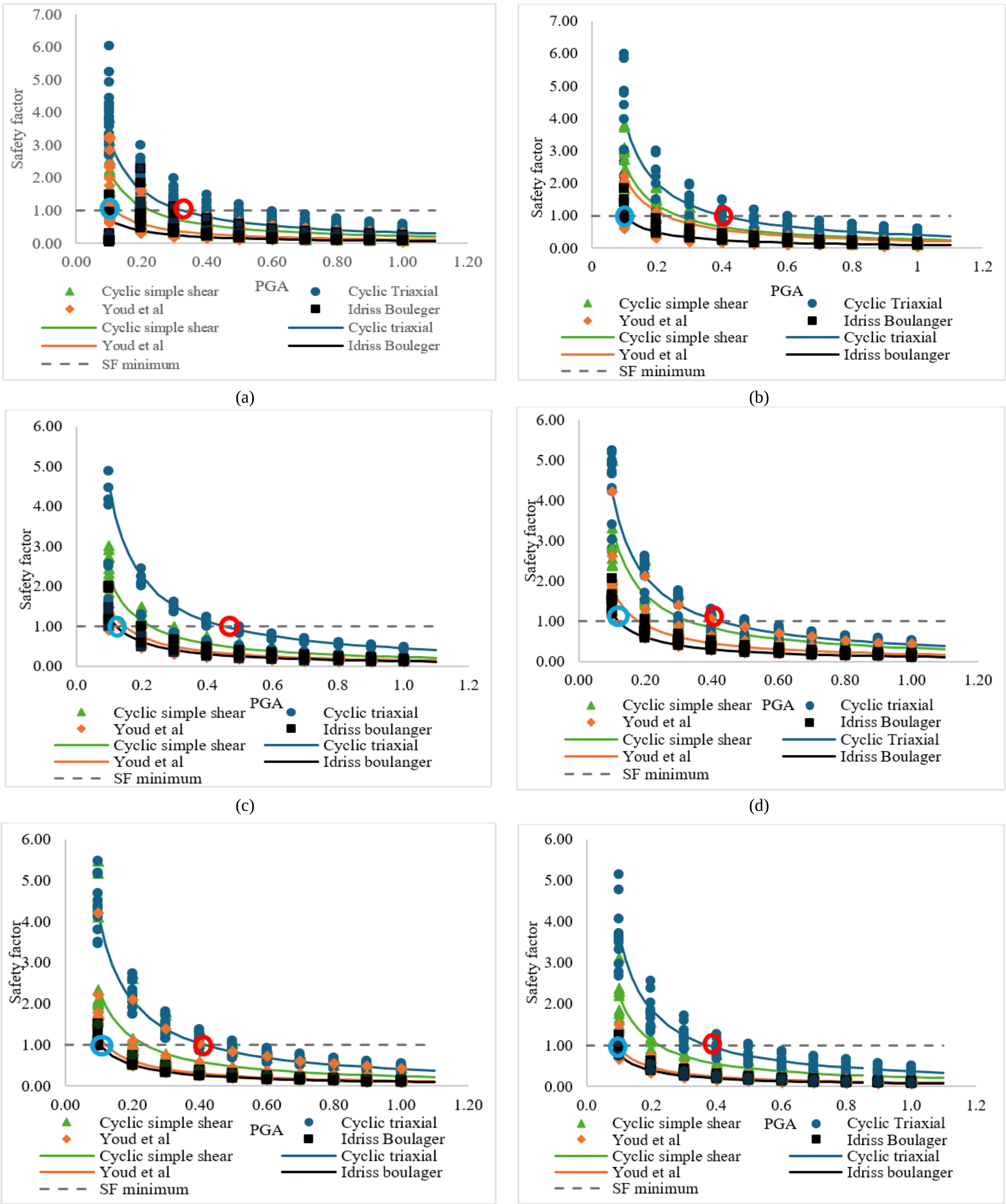

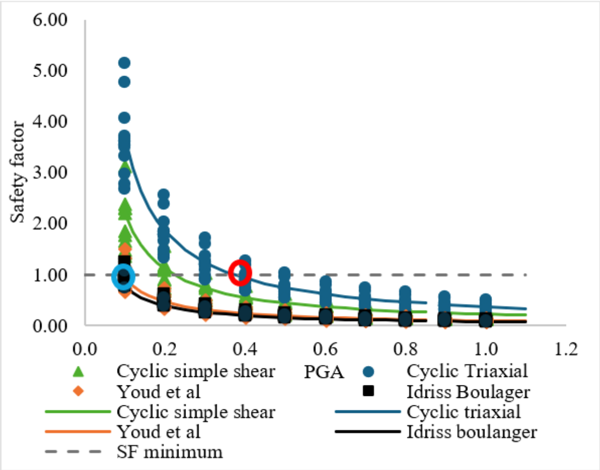

(g)

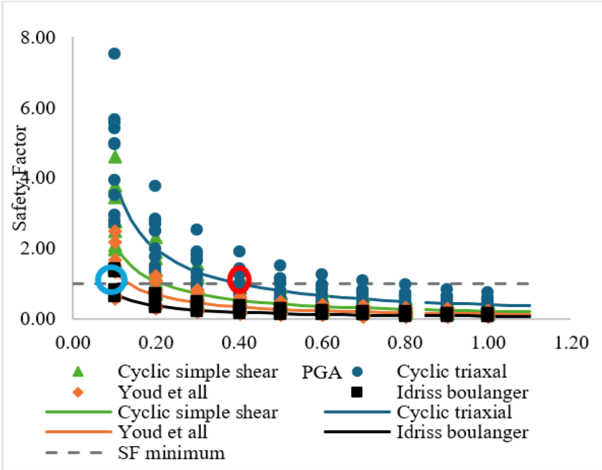

(h)

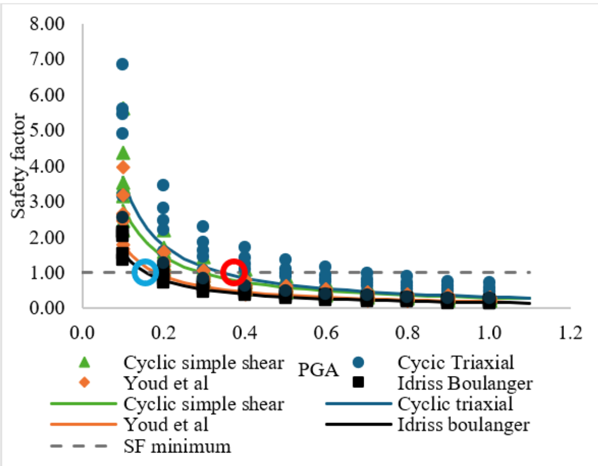

(i)

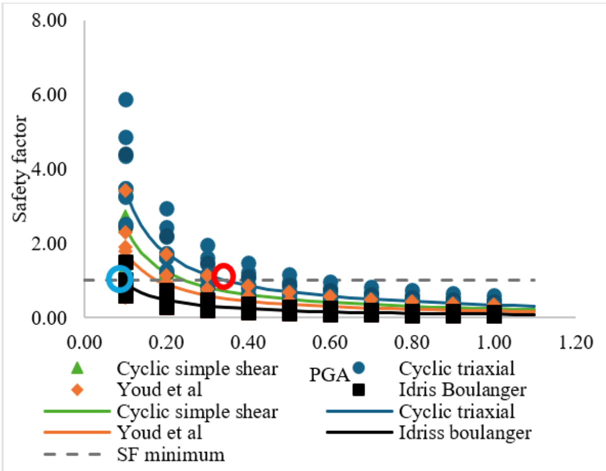

(j)

Figure 8. Safety factor against Peak Ground acceleration (PGA) (a) Location 1, (b) Location 2, (c) Location 3, (d) Location 4, (e) Location 5, (f) Location 6, (g) Location 7, (h) Location 8, (i) Location 9, and (j) Location 10

The entire location shows that the PGA ranges from 0.5 to 1.0 (g), and the curve depicts the asymptotes output. The empirical approach shows the narrow range of FS through the differences in PGA, whereas the element simulation provides more significant range differences, which means that the empirical method always generates more conservative results, although it provides an overestimated design for the structure at once. The significant gap output in the elemental simulation ranges from 0.1 to 0.3 g in every action (blue and red circle mark); the engineer must consider a specific PGA value to produce the optimal estimation. The marks in different colors indicate the minimum and maximum threshold of the PGA with FS=1. A summary of the ranges between the minimum and maximum border of the FS against the PGA for all locations is presented in Table 3.

Table 3. PGA consideration

Area	Minimum PGA range(g)	Maximum PGA range (g)
Lombok	0.1	0.42-0.45
Yogyakarta	0.1-0.12	0.4-0.45
Palu	0.1-0.15	0.35-0.40

In general, minimum liquefaction occurs at a PGA of 1.5 g, which is the minimum threshold of the Japanese design codes. This study shows that the empirical methods produce a PGA range of approximately 0.1–0.15 g to obtain the FS value at 1.0. For a PGA of 0.1 g, all locations depicted the FS from CXT results approximately five times greater than the approach of Idriss & Boulanger [27]; in comparison with Youd & Idriss (2001) [28], the differences were slightly lower. This difference gradually declines until it is asymptotic, and the FS from the CXT output tends to decrease dramatically until the PGA is approximately 0.35g. These conditions indicated conservative results from the empirical method for low PGA values. Although the suggested turning value is in PGA of approximately 0.35g, Filali & Sbartai [57] suggested a nonlinear dynamic method to verify the liquefaction analysis with PGA conditions exceeding 0.3g.

According to Table 3, the minimum value of PGA from all locations (empirical Idriss-Boulanger) is in the range of 0.1–0.15 g PGA. The calculated FS is underestimated depending on a PGA consideration; in another research location (excluding Indonesia), the soil model was determined to be secure from liquefaction, with a particular PGA value of 0.18 to 0.16 g [58, 59]. In addition, the value shown in the constitutive model in the element simulation (CXT simulation) is higher, with a range of 0.35–0.45 g, whereas the probability of liquefaction was 65–85% for the PGA range of 0.6–0.75 g. The CXT and CSS simulations provided adequate performance compared with the empirical method for all locations. An undercalculated FS leads to an overestimated design to prevent the liquefaction effect, which results in high costs and overestimation [59].

The soil profiles of Indonesian regions frequently vary and are complex, consisting of alternating layers of organic substances, clay, and sediment. This heterogeneity presents a challenge in accurately estimating the PL using a simplified method [60]. Moreover, the accuracy of PL estimates may be affected by the absence of comprehensive region-specific geotechnical information for many areas in Indonesia. However, this information can be acquired by employing methodologies developed for other geological conditions. A simple standard for soil liquefaction vulnerability in Indonesia does not fully cover the complexity of liquefaction assessment. This study only considered cyclic soil elements as an alternative, and other methods, such as nonlinear dynamic analysis, can also be used for extensive liquefaction assessment [57].

A variant PGA value was calculated to determine the PGA threshold for liquefaction. In Christchurch, liquefaction occurred during the 2010–2011 Canterbury earthquake sequence, with a maximal acceleration of approximately 0.08 g [61]. Limited liquefaction was observed in Italy following the 2009 L'Aquila earthquake [62], with an estimated PGA of 0.065g on the outcropping bedrock. Hence, because the history and recommendations of past research show different PGA thresholds, it is crucial to consider the site-specific characteristics of intense ground motions and soil properties to make a valid assessment of liquefaction regarding potential future large earthquakes [63].

3.4. Validation Data for Specific Area Based on Probabilistic Calculations

The range of PGA in the FS calculation variants leads to a critical value for the liquefaction potential in several approaches. Moreover, the deterministic approach uses FS as the dependent value for assessing site condition. In contrast, the probabilistic approach offers site conditions predicted in different ranges. A specific description of the PL is provided in Table 2. The equal chance situation between the non-liquefaction and liquefaction conditions is at the border or PL 0.65, which indicates the threshold condition of the liquefaction potential effect. As a validation assessment through deterministic analyses that depend on the PGA recommendation threshold, a probabilistic calculation was conducted to compare the liquefaction potential with the maximum PGA recommendations in Table 3. The output of the data distribution is shown in Figure 9.

As the variable mentioned in the methodology section, the area has the specific PGA value from the Indonesia Hazard map, namely 0.3-0.46g for the Lombok area, 0.46g for the Yogyakarta area, and 0.6g for Palu. In contrast, the PGA threshold recommendation in Table 3 reaches a maximum of 0.4-0.45 g. This implies that the Yogyakarta area is almost exactly at the border of the PGA, the Lombok area is under the PGA recommendation, and the Palu area is above the threshold.

As shown in Figure 9, soil sample data with a PL value under 0.65, which means that they were unlikely to experience liquefaction, were examined in the Lombok, Yogyakarta, and Palu areas. In the Lombok area, 43% of data had PL value< 0.65. The liquefaction ratio was dominated by CXT, CSS, and Youd & Idriss (2001) [28]; only 5% of Idris & Boulanger's [27] calculations had a PL of less than 0.65. Contrastingly, in the Yogyakarta area, the PL under 0.65 reaches 33.3%, with CXT and CSS in large percentages, and Youd & Idriss (2001) [28] calculation in 8.3%. Regarding the Palu area, the PL <0.65 only obtained 6.8% of the CXT simulation. This means that smaller inputs of PGA, CXT, and CSS play a significant role in determining the threshold of maximum acceleration, which leads to safe conditions. The minimum value of the PGA provides a large gap between the empirical method and the CXT and CSS simulations. The condition of the PGA under the recommendation shows that the element simulation can achieve almost half of the data for safe conditions. These circumstances indicate the overestimation of the empirical approach in liquefaction potential prediction. Thus, following Franke et al. [64], in regions that have slight to moderate seismic activity, a more precise probabilistic seismic hazard analysis can assist in minimizing overestimation for soil liquefaction analysis. This necessitates a more accurate assessment of seismic impacts in accordance with site conditions.

The output provides an overestimation of the simplified method for assessing liquefaction in a particular PGA range. According to Möller et al. [43], various liquefaction approaches overestimate soil resistance under large-amplitude dynamic loading while underestimating its strength during low-amplitude loading. Furthermore, as with other semi-empirical methodologies, the Idriss & Boulanger [27] approach is deliberately conservative in accommodating uncertainties in actual conditions and variations in soil characteristics. The cyclic resistance of all soil types may not always be accurately represented by these correlations, which may generate a conservative calculation [65-67].

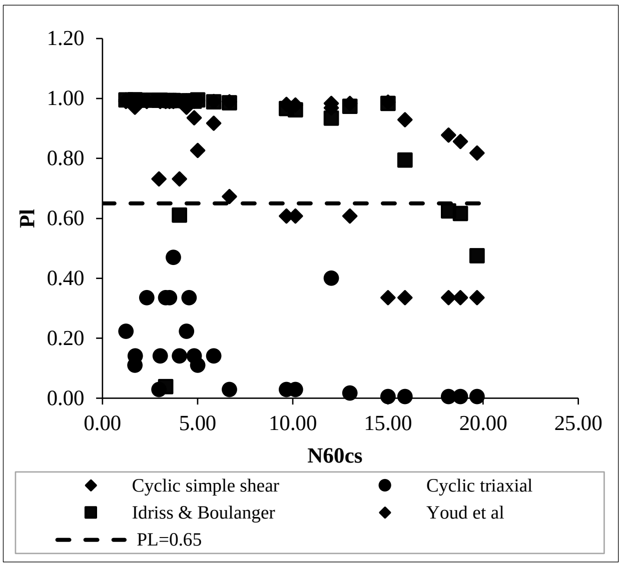

(a)

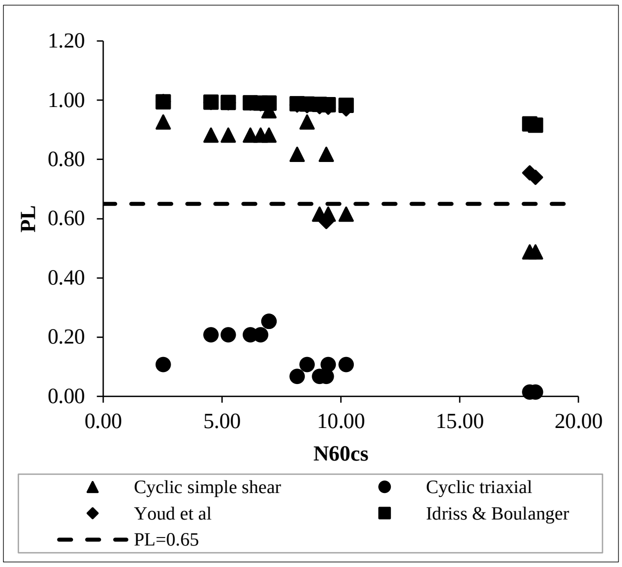

(b)

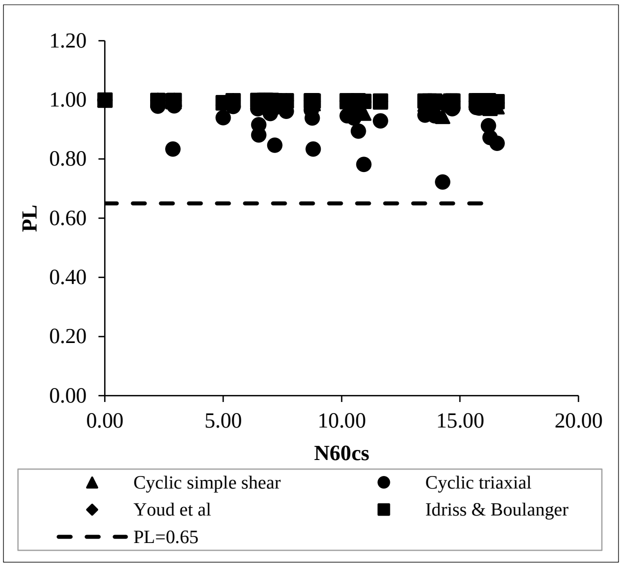

(c)

Figure 9. Liquefaction probabilistic calculation output (a) Lombok area (b) Yogyakarta area (c) Palu area

This study utilized a validation range with a probabilistic approach because this method provides a greater chance of the data validation than deterministic analysis in Bangladesh [65]. Although the result shows that PGA of 0.45 gives the maximum threshold of liquefaction potential analysis between empirical and element simulations, another complicated relationship between local geological, hydrogeological, and geotechnical characteristics should be determined to comprehend variations in liquefaction at varying depths and locations [69]. Hence, the general recommendation from this research is expected to provide an ideal proposal for determining liquefaction ratios from laboratory data based on cyclic tests or element simulations to prevent the overestimation of the empirical method. Although the simplified method is convenient and applicable in engineering practice, the Indonesian standard of geotechnical assessments should consider soil sample data to comprehensively assess liquefaction.

4. Conclusion

This study used a soil element simulation based on LIQCA to obtain the liquefaction ratios in the CXT and CSS. In addition, the empirical methods of Idriss & Boulanger (2008) [27] and Youd & Idriss (2001) [28] were used to combine the CXT and CSS. A statistically significant correlation was observed between CXT and CSS. This research shows a strong connection between $(N_1)_{60cs}$ and the strength ratio. Although CXT offers the highest liquefaction strength ratio in all methods, the Pearson correlation range is not sufficient, with 0.6–0.88. Furthermore, the more data collected, the more negligible the Pearson correlation in the empirical method of Idriss & Boulanger's (2008) [27], despite providing the satisfactory data distribution almost constantly in all locations. In the low N SPT value, the range between the CSS and empirical is narrower than that in the more considerable condition. Both the CXT and CSS empirical calculations show the various values of the strength-based approaches used in liquefaction assessments.

In the deterministic approach, the FS was obtained from the various simulations of the threshold of these parameters. Various minimum PGAs are obtained with FS=1 in the empirical method, whereas CXT plays a significant role in the maximum PGA with the same FS value. The maximum recommendation range is 0.350–0.45 g, while the minimum is 0.1–0.15 g from empirical approaches. This indicates an overestimation by the empirical method. In addition, the probabilistic approach proves that the PL with a 0.65 threshold of the PGA under the recommendation threshold reaches 43% of the data distribution in the safe condition. Hence, combining cyclic tests and empirical methods produces a comprehensive and optimal target for analyzing liquefaction vulnerability in Indonesia.

5. Declarations

5.1. Author Contributions

Conceptualization, F.S.N. and S.K.; methodology, F.S.N.; software, F.S.N.; validation, F.S.N. and S.K.; formal analysis, S.K.; investigation, F.S.N.; resources, F.S.N.; data curation, S.K.; writing—original draft preparation, F.S.N.; writing—review and editing, F.S.N. and S.K.; visualization, F.S.N.; supervision, S.K.; project administration, S.K.; funding acquisition, S.K. All authors have read and agreed to the published version of the manuscript.

5.2. Data Availability Statement

Data sharing is not applicable to this article.

5.3. Funding

This research is the part of doctoral thesis funded by Japanese Government Scholarship (Monbukagakusho/MEXT) Scholarships.

5.4. Acknowledgements

Authors express our sincere gratitude for the funding by Japanese Government Scholarship (Monbukagakusho / MEXT), PT. Wijaya Karya for secondary soil data project in Indonesia, Associate Professor Yoshikawa Takahiro from Gifu university and Associate Professor Yokawa Hiroshi from Chubu university that give valuable comment and information.

5.5. Conflicts of Interest

The authors declare no conflict of interest.

6. References

[1] Zulfakriza, Z., Nugraha, A. D., Heryandoko, N., Ry, R. V., Muttaqy, F., Andika, A., Azhari, M. F., Putra, A. S., Palgunadi, K. H., Cummins, P. R., Supendi, P., Lesmana, A., Sahara, D. P., & Puspito, N. T. (2024). Seismic source analysis of the destructive earthquake November 21, 2022, Mw 5.6 Cianjur (Indonesia) from relocated aftershock. Scientific Reports, 14(1), 12142. doi:10.1038/s41598-024-60408-9.

[2] Supendi, P., Winder, T., Rawlinson, N., Bacon, C. A., Palgunadi, K. H., Simanjuntak, A., Kurniawan, A., Widiyantoro, S., Nugraha, A. D., Shiddiqi, H. A., Ardianto, Daryono, Adi, S. P., Karnawati, D., Priyobudi, Marliyani, G. I., Imran, I., & Jatnika, J. (2023). A conjugate fault revealed by the destructive Mw 5.6 (November 21, 2022) Cianjur earthquake, West Java, Indonesia. Journal of Asian Earth Sciences, 257, 105830. doi:10.1016/j.jseaes.2023.105830.

[3] Nurlita Fitri, S., Asih Aryani Soemitro, R., Dewa Warnana, D., & Sutra, N. (2018). Application of microtremor HVSR method for preliminary assessment of seismic site effect in Ngipik landfill, Gresik. MATEC Web of Conferences, 195. doi:10.1051/matecconf/201819503017.

[4] Purwana, Y. M., Goro, G. L., Fitri, S. N., Setiawan, B., & Arbianto, R. (2022). Assessment of Seismic Loss in Surakarta School Buildings. Civil Engineering and Architecture, 10(5), 1772–1787. doi:10.13189/cea.2022.100506.

[5] Kusumawardani, R., Chang, M., Upomo, T. C., Huang, R. C., Fansuri, M. H., & Prayitno, G. A. (2021). Understanding of Petobo liquefaction flowslide by 2018.09.28 Palu-Donggala Indonesia earthquake based on site reconnaissance. Landslides, 18(9), 3163–3182. doi:10.1007/s10346-021-01700-x.

[6] Tanjung, M. I., Irsyam, M., Sahadewa, A., Iai, S., Tobita, T., & Nawir, H. (2023). Overview of Flowslide in Petobo during liquefaction of the 2018 Palu Earthquake. Soil Dynamics and Earthquake Engineering, 173. doi:10.1016/j.soildyn.2023.108110.

[7] Geological Department. (2019). ATLAS Liquefaction vulnerability zone in Indonesia. Ministry of Energy and Mineral Resource, Bandung, Indonesia. (In Indonesian).

[8] Cilia, M. G., Mooney, W. D., & Nugroho, C. (2021). Field Insights and Analysis of the 2018 Mw 7.5 Palu, Indonesia Earthquake, Tsunami and Landslides. Pure and Applied Geophysics, 178(12), 4891–4920. doi:10.1007/s00024-021-02852-6.

[9] Kiyota, T., Furuichi, H., Hidayat, R. F., Tada, N., & Nawir, H. (2020). Overview of long-distance flow-slide caused by the 2018 Sulawesi earthquake, Indonesia. Soils and Foundations, 60(3), 722–735. doi:10.1016/j.sandf.2020.03.015.

[10] Nanda, G. I., & Mulyani, A. (2021). Analysis of landscape changes using high-resolution satellite images at former rice fields after earthquake and liquefaction in Central Sulawesi Province. IOP Conference Series: Earth and Environmental Science, 648(1), 012203. doi:10.1088/1755-1315/648/1/012203.

[11] Mase, L. Z. (2017). Experimental liquefaction study of Southern Yogyakarta using shaking table. Journal of Civil Engineering, 23(1), 11-18.

[12] Tsimopoulou, V., Mikami, T., Hossain, T. T., Takagi, H., Esteban, M., & Utama, N. A. (2020). Uncovering unnoticed small-scale tsunamis: field survey in Lombok, Indonesia, following the 2018 earthquakes. Natural Hazards, 103(2), 2045–2070. doi:10.1007/s11069-020-04071-z.

[13] National Academies of Sciences, Engineering, and Medicine. (2021). State of the art and practice in the assessment of earthquake-induced soil liquefaction and its consequences. National Academy of Sciences, Washington, United States. doi:10.17226/23474.

[14] Fitri, S. N., & Sawada, K. (2024). Evaluation and Opportunities for Soil Liquefaction Vulnerability Research: Lesson Learned from Japan for Indonesia - A Bibliometric Analysis. Proceedings of the 2024 11th International Conference on Geological and Civil Engineering, ICGCE 2024, Springer Series in Geomechanics and Geoengineering, Springer, Cham, Switzerland. doi:10.1007/978-3-031-68624-5_2.

[15] SNI 8460-2017. (2017). Geotechnical Design Requirements. Badan Standarisasi Nasional, Jakarta, Indonesia. (In Indonesian).

[16] Seed, H. B., & Idriss, I. M. (1971). Simplified procedure for evaluating soil liquefaction potential. Journal of the Soil Mechanics and Foundations division, 97(9), 1249-1273. doi:10.1061/JSFEAQ.0001662.

[17] Ye, B., Ye, G., Zhang, F., & Yashima, A. (2007). Experiment and numerical simulation of repeated liquefaction-consolidation of sand. Soils and Foundations, 47(3), 547–558. doi:10.3208/sandf.47.547.

[18] Oka, F., Yashima, A., Tateishi, A., Taguchi, Y., & Yamashita, S. (1999). A cyclic elasto-plastic constitutive model for sand considering a plastic-strain dependence of the shear modulus. Geotechnique, 49(5), 661–680. doi:10.1680/geot.1999.49.5.661.

[19] The LIQCA Research and Development Group (2009). User's manual for LIQCA2D09. Representative: Oka, F. of Kyoto University, Kyoto, Japan.

[20] Nishimura, S. (2022). Application of Probabilistic Models to Material Strength, Structural Strength and Disaster Occurrence. Journal of the Society of Materials Science, Japan, 71(2), 197–203. doi:10.2472/jsms.71.197.

[21] Kato, K., Nagao, K., & Suemasa, N. (2019). Numerical simulation of undrained cyclic behavior for desaturated silica sands. Japanese Geotechnical Society Special Publication, 7(2), 505–515. doi:10.3208/jgssp.v07.080.

[22] Kuribayashi, K., Hara, T., Sakabe, A., & Kuroda, S. (2021). A Study on Damages of Road Embankment on the Liquefaction Ground. Journal of Japan Association for Earthquake Engineering, 21(1), 1_46-1_63. doi:10.5610/jaee.21.1_46.

[23] Santucci de Magistris, F., Lanzano, G., Forte, G., & Fabbrocino, G. (2013). A database for PGA threshold in liquefaction occurrence. Soil Dynamics and Earthquake Engineering, 54, 17–19. doi:10.1016/j.soildyn.2013.07.011.

[24] Jalil, A., Fathani, T. F., Satyarno, I., & Wilopo, W. (2021). Liquefaction in Palu: the cause of massive mudflows. Geoenvironmental Disasters, 8(1). doi:10.1186/s40677-021-00194-y.

[25] Aini, I., Wilopo, W., & Fathani, T. F. (2024). Development of Peak Ground Acceleration Using a Non-Linear Approach To Evaluate Liquefaction Potential in Sei Wampu Bridge, Langkat, North Sumatra, Indonesia. ASEAN Engineering Journal, 14(3), 41–52. doi:10.11113/aej.V14.20606.

[26] Zakariya, A., Rifaí, A., & Ismanti, S. (2023). Comparative Analysis of Quantitative Indices for Evaluating the Liquefaction Potential of Medium-Dense Cohesionless Soil. Journal of GeoEngineering, 18(3), 93–102. doi:10.6310/jog.202309_18(3).1.

[27] Idriss, I. M., & Boulanger, R. W. (2008). Soil liquefaction during earthquakes. Earthquake Engineering Research Institute, Oakland, United States.

[28] Youd, T. L., & Idriss, I. M. (2001). Liquefaction Resistance of Soils: Summary Report from the 1996 NCEER and 1998 NCEER/NSF Workshops on Evaluation of Liquefaction Resistance of Soils. Journal of Geotechnical and Geoenvironmental Engineering, 127(4), 297–313. doi:10.1061/(asce)1090-0241(2001)127:4(297).

[29] Zakariya, A., Rifa'I, A., & Ismanti, S. (2023). Ground Motion and Liquefaction Study at Opak River Estuary Bantul. IOP Conference Series: Earth and Environmental Science, 1244(1). doi:10.1088/1755-1315/1244/1/012032.

[30] Irdhiani, Rifa'i, A., Fathani, T. F., & Adi, A. D. (2024). Post-Earthquake Liquefaction Vulnerability Mapping by Swedish Weight Sounding and Standard Penetration Test. Civil Engineering Journal (Iran), 10(7), 2216–2232. doi:10.28991/CEJ-2024-010-07-09.

[31] Kiyota, T., Shiga, M., Katagiri, T., Furuichi, H., & Nawir, H. (2022). Effect of Artesian Pressure on Liquefaction-Induced Flow-Slide: A Case Study of the 2018 Sulawesi Earthquake, Indonesia. Geotechnical, Geological and Earthquake Engineering, 52, 1579–1586. doi:10.1007/978-3-031-11898-2_140.

[32] Mase, L. Z. (2017). Shaking table test of soil liquefaction in southern Yogyakarta. International Journal of Technology, 8(4), 747–760. doi:10.14716/ijtech.v8i4.9488.

[33] Khashila, M., Hussien, M. N., Karray, M., & Chekired, M. (2021). Liquefaction resistance from cyclic simple and triaxial shearing: a comparative study. Acta Geotechnica, 16(6), 1735–1753. doi:10.1007/s11440-020-01104-6.

[34] Rodriguez-Arriaga, E., & Green, R. A. (2018). Assessment of the cyclic strain approach for evaluating liquefaction triggering. Soil Dynamics and Earthquake Engineering, 113, 202–214. doi:10.1016/j.soildyn.2018.05.033.

[35] Önalp, A., Özocak, A., Bol, E., Sert, S., Arslan, E., & Ural, N. (2024). An investigation into dynamic behaviour of reconstituted and undisturbed fine-grained soil during triaxial and simple shear. Bulletin of Earthquake Engineering, 22(11), 5599–5618. doi:10.1007/s10518-024-01980-3.

[36] Oka, F., Oshima, A., & Fukai, H. (2023). Evaluation of liquefaction strength of Japanese natural sandy soil using triaxial and simple shear tests. Soils and Foundations, 63(4). doi:10.1016/j.sandf.2023.101349.

[37] Sternik, K. (2024). Static liquefaction as a form of material instability in element test simulations of granular soil. Archives of Civil Engineering, 70(2), 309–322. doi:10.24425/ace.2024.149865.

[38] Fujiwara, K., Ogawa, N., & Nakai, K. (2021). 3-D Numerical Analysis of Partial Floating Sheet-Pile Method as Countermeasure for Liquefaction. Journal of JSCE, 9(1), 138–147. doi:10.2208/journalofjsce.9.1_138.

[39] Santucci de Magistris, F., Lanzano, G., Forte, G., & Fabbrocino, G. (2014). A peak acceleration threshold for soil liquefaction: lessons learned from the 2012 Emilia earthquake (Italy). Natural Hazards, 74(2), 1069–1094. doi:10.1007/s11069-014-1229-x.

[40] BNBP (2017). Indonesian Seismic Sources and Seismic Hazard Maps: Center for research and development of housing and resettlement. Ministry of Public Works and Human Settlements, National Center for Earthquake Studies, Jakarta, Indonesia.

[41] Orense, R. P. (2005). Assessment of liquefaction potential based on peak ground motion parameters. Soil Dynamics and Earthquake Engineering, 25(3), 225–240. doi:10.1016/j.soildyn.2004.10.013.

[42] Mase, L. Z., Fathani, T. F., & Adi, A. D. (2021). A simple shaking table test to measure liquefaction potential of Prambanan Area, Yogyakarta, Indonesia. ASEAN Engineering Journal, 11(3), 89-108. doi:10.11113/aej.v11.16874.

[43] Möller, J. K., Taborda, D. M. G., Kontoe, S., & Potts, D. M. (2024). A shear history model for capturing the liquefaction resistance of sands at various cyclic stress ratios. Computers and Geotechnics, 166. doi:10.1016/j.compgeo.2023.105940.

[44] Juang, C. H., Ching, J., Luo, Z., & Ku, C. S. (2012). New models for probability of liquefaction using standard penetration tests based on an updated database of case histories. Engineering Geology, 133–134, 85–93. doi:10.1016/j.enggeo.2012.02.015.

[45] Chen, C. J., & Juang, C. H. (2000). Calibration of SPT- and CPT-based liquefaction evaluation methods. Proceedings of Sessions of Geo-Denver 2000 - Innovations and Applications in Geotechnical Site Characterization, GSP 97, 285, 49–64. doi:10.1061/40505(285)4.

[46] Porcino, D., Marcianò, V., & Granata, R. (2011). Undrained cyclic response of a silicate-grouted sand for liquefaction mitigation purposes. Geomechanics and Geoengineering, 6(3), 155–170. doi:10.1080/17486025.2011.560287.

[47] Wu, J., Kammerer, A. M., Riemer, M. F., Seed, R. B., & Pestana, J. M. (2004). Laboratory study of liquefaction triggering criteria. 13th World Conference on Earthquake Engineering, 1-6 August, Vancouver, Canada.

[48] Nong, Z. Z., Park, S. S., & Lee, D. E. (2021). Comparison of sand liquefaction in cyclic triaxial and simple shear tests. Soils and Foundations, 61(4), 1071–1085. doi:10.1016/j.sandf.2021.05.002.

[49] Artati, H., Pawirodikromo, W., Rahardjo, P., & Makrup, L. (2023). Effect of Fines Content on Liquefaction Resistance During Steady-State Conditions. International Journal of GEOMATE, 25(109), 18–28. doi:10.21660/2023.109.3481.

[50] Idriss, I. M., & Boulanger, R. W. (2010). SPT-based liquefaction triggering procedures. Report No. UCD/CGM-10, 2, Center for Geotechnical Modeling, Department of Civil and Environmental Engineering, University of California, Davis, United States.

[51] Mandokhail, S. ullah J., Park, D., & Yoo, J. K. (2017). Development of normalized liquefaction resistance curve for clean sands. Bulletin of Earthquake Engineering, 15(3), 907–929. doi:10.1007/s10518-016-0020-7.

[52] Boulanger, R. W., & Idriss, I. M. (2012). Probabilistic Standard Penetration Test–Based Liquefaction–Triggering Procedure. Journal of Geotechnical and Geoenvironmental Engineering, 138(10), 1185–1195. doi:10.1061/(asce)gt.1943-5606.0000700.

[53] Chen, G., Xu, L., Kong, M., & Li, X. (2015). Calibration of a CRR model based on an expanded SPT-based database for assessing soil liquefaction potential. Engineering Geology, 196, 305–312. doi:10.1016/j.enggeo.2015.08.002.

[54] Tripathi, C. B., Jha, P. K., & Agarwal, R. (2024). Method comparison: Statistical measurement correlation or agreement-most appropriate tool? Asian Journal of Medical Sciences, 15(1), 262–268. doi:10.3126/ajms.v15i1.58213.

[55] Hanindya, K. A., Makrup, L., Widodo, & Paulus, R. (2023). Deterministic Seismic Hazard Analysis to Determine Liquefaction Potential Due to Earthquake. Civil Engineering Journal (Iran), 9(5), 1203–1216. doi:10.28991/CEJ-2023-09-05-012.

[56] Bhutani, M., & Naval, S. (2020). Assessment of seismic site response and liquefaction potential for some sites using borelog data. Civil Engineering Journal (Iran), 6(11), 2103–2119. doi:10.28991/cej-2020-03091605.

[57] Filali, K., & Sbartai, B. (2017). A comparative study between simplified and nonlinear dynamic methods for estimating liquefaction potential. Journal of Rock Mechanics and Geotechnical Engineering, 9(5), 955–966. doi:10.1016/j.jrmge.2017.05.008.

[58] Towhata, I., Wu, W., & Borja, R. I. (2008). Geotechnical Earthquake Engineering. Springer Series in Geomechanics and Geoengineering, 1. doi:10.2113/gseegeosci.iii.1.158.

[59] Poddar, P., Ojha, S., & Gupta, M. K. (2023). Probabilistic and deterministic-based approach for liquefaction potential assessment of layered soil. Natural Hazards, 118(2), 993–1012. doi:10.1007/s11069-023-06031-9.

[60] Jalil, A., Fathani, T. F., Satyarno, I., & Wilopo, W. (2020). A study on the liquefaction potential in Banda Aceh city after the 2004 sumatera earthquake. International Journal of GEOMATE, 18(65), 147–155. doi:10.21660/2020.65.94557.

[61] Quigley, M. C., Bastin, S., & Bradley, B. A. (2013). Recurrent liquefaction in Christchurch, New Zealand, during the Canterbury earthquake sequence. Geology, 41(4), 419–422. doi:10.1130/G33944.1.

[62] Monaco, P., de Magistris, F. S., Grasso, S., Marchetti, S., Maugeri, M., & Totani, G. (2011). Analysis of the liquefaction phenomena in the village of Vittorito (L'Aquila). Bulletin of Earthquake Engineering, 9(1), 231–261. doi:10.1007/s10518-010-9228-0.

[63] Hata, Y., Ichii, K., Nozu, A., Maruyama, Y., & Sakai, H. (2013). Ground motion estimation at the farthest liquefaction site during the 2011 off the pacific coast of Tohoku earthquake. Soil Dynamics and Earthquake Engineering, 48, 132–142. doi:10.1016/j.soildyn.2013.01.002.

[64] Franke, K. W., Lingwall, B. N., Youd, T. L., Blonquist, J., & Liang, J. H. (2019). Overestimation of liquefaction hazard in areas of low to moderate seismicity due to improper characterization of probabilistic seismic loading. Soil Dynamics and Earthquake Engineering, 116, 681–691. doi:10.1016/j.soildyn.2018.10.040.

[65] Berkat, B., Akhssas, A., Ouadif, L., & Bahi, A. (2024). Assessment of Liquefaction Potential by Comparing Semi-Empirical Methods Based on the CPT Test. Civil and Environmental Engineering, 20(1), 164-179. doi:10.2478/cee-2024-0014.

[66] Touijrate, S., Baba, K., Ahatri, M., & Bahi, L. (2018). Validation and Verification of Semi-Empirical Methods for Evaluating Liquefaction Using Finite Element Method. MATEC Web of Conferences, 149, 02028. doi:10.1051/matecconf/201814902028.

[67] Idriss, I. M., & Boulanger, R. W. (2006). Semi-empirical procedures for evaluating liquefaction potential during earthquakes. Soil Dynamics and Earthquake Engineering, 26(2-4 SPEC. ISS.), 115–130. doi:10.1016/j.soildyn.2004.11.023.

[68] Berkat, B., Akhssas, A., & Elfilali, O. (2024). Assessing Liquefaction Potential in Alluvial Plains through Spatiotemporal Analysis Using Liquefaction Probability Index. Civil Engineering Journal (Iran), 10(6), 2007–2018. doi:10.28991/CEJ-2024-010-06-018.